RSC Advances

PAPER

Cite this: *RSC Adv.*, 2015, **5**, 11334

pH-responsive host–guest polymerization and blending†

Daniele Masseroni,[a] Enrico Rampazzo,[b] Federico Rastrelli,[c] Davide Orsi,[d] Lucia Ricci,[e] Giacomo Ruggeri[e] and Enrico Dalcanale*[a]

In this work, we demonstrate – in two different settings – the potential of the recognition motif made by tetraphosphonate cavitand/*N*-methyl ammonium salt for the development of supramolecular polymer chemistry. In the first part a novel pH sensitive supramolecular homopolymer was assembled by proper design of the corresponding monomer, and monitoring the self-assembling process by several analytical tools, including NMR spectroscopy and light scattering techniques. These measurements provided the evidence for the formation of the homopolymer and its pH responsiveness. In the second study, the two recognition groups – tetraphosphonate cavitand (Host) and sarcosine hydrochloride (Sarc) – introduced in polystyrene (PS–Host) and poly(butyl methacrylate) (PBMA–Sarc) respectively, led to the mixing of the two otherwise immiscible polymers thanks to the energetically favourable host–guest interactions between the polymer chains. The polymer blending was verified by the presence of a single glass transition temperature (T_g) and showed its homogeneous morphology by atomic force microscopy (AFM).

Received 18th November 2014
Accepted 12th January 2015

DOI: 10.1039/c4ra14793f

www.rsc.org/advances

Introduction

Challenges in polymer science have increased in recent years thanks to a growing demand for new functional materials presenting a wide range of properties, such as the self-healing to mechanical stress and the ability to reversibly adapt to external stimuli.[1] Supramolecular polymer chemistry addresses the multifaceted tasks of designing smart materials and expanding polymer applications through the rational implementation of non-covalent interactions in polymer chemistry.[2,3] The nature of the secondary weak interactions and the types of building blocks involved in the supramolecular polymer systems are pivotal to determine the responsiveness of the resulting materials. In this context, host–guest chemistry can offer a palette of non-covalent interactions, within a large variety of interacting species. Molecular receptors such as cyclodextrins,[4] cucurbiturils,[5–7] calixarenes,[8,9] crown ethers[10,11] and pillararenes[12] are ideal components of supramolecular polymers thanks to their synthetic and binding versatility. Moreover the host–guest interactions endow the final supramolecular materials with some attractive features like stimuli responsiveness to pH, temperature, electrons and light.[13–15] A further class of molecular receptors that fulfils the requirement of high association constants necessary for polymerization is the one of tetraphosphonate cavitands (Tiiii).[16,17] These resorcinarene based cavitands functionalized at the upper rim with four phosphonate groups – oriented inward with respect to the cavity – are appealing receptors thanks to remarkable recognition properties towards positively charged species. In particular the ability of tetraphosphonate cavitands to recognize the *N*-alkyl ammonium hydrochloride moieties have been demonstrated by our group in several papers including the complexation of the series of *N*-alkyl ammonium salts,[18] for molecules of biological interest like sarcosine[19] and the antitumor drug procarbazine hydrochloride.[20] The observed selectivity is the results of the synergic action of three interaction modes: (i) multiple ion–dipole interactions between the inward facing P=O groups and the positively charged guest;[21] (ii) hydrogen bonding interactions between the $-NH_2$ group of the guest and the phosphonate groups;[22] (iii) CH–π interaction involving the methyl group of the guest and the electron rich cavity of the receptor.[23] The high association constants and pH dependence of the tetraphosphonate cavitand/*N*-methyl ammonium complexes prompted us to use them as building block to construct new supramolecular materials. Herein, we report the relevance of such host–guest interaction to form reversible supramolecular polymers and blends.

[a]*Dipartimento di Chimica and INSTM, UdR Parma, Università di Parma, Viale delle Scienze 17/A, 43124 Parma, Italy. E-mail: enrico.dalcanale@unipr.it*

[b]*Dipartimento di Chimica "G. Ciamician" and INSTM, UdR Bologna, Università di Bologna, Via Selmi 2, 40126 Bologna, Italy*

[c]*Dipartimento di Scienze Chimiche, Università degli Studi di Padova, Via Marzolo 1, 35131 Padova, Italy*

[d]*Dipartimento di Fisica, Università di Parma, Viale delle Scienze 7/A, 43124 Parma, Italy*

[e]*Dipartimento di Chimica e Chimica Industriale and INSTM, UdR Pisa, Università di Pisa, Via Giuseppe Moruzzi 3, 56124 Pisa, Italy*

† Electronic supplementary information (ESI) available: Homopolymer characterization, ITC of host–guest complex, experimental and characterization details of PBMA–Sarc, DSC and NMR analyses of PS–Host/PBMA–Sarc blend. See DOI: 10.1039/c4ra14793f

In the first part of the work a new pH dependent supramolecular homopolymer was self-assembled. An AB-type self-complementary heteroditopic monomer based on tetraphosphonate cavitand was synthesized introducing a sarcosine moiety at the lower rim of the receptor. In this case the supramolecular polymerization was promoted by the complexation of the protonated secondary amine by the tetraphosphonate cavitand. The pH dependence of the polymerization was demonstrated using several complementary techniques, such as ^{1}H and ^{31}P NMR spectroscopy, NMR diffusometry (DOSY) and light scattering measurements.

In the second section of the paper the molecular recognition properties of the supramolecular complex were used to introduce supramolecular cross-links and, in turn, to induce the compatibilization of two immiscible polymers: polystyrene (PS) and poly(butyl methacrylate) (PBMA). Indeed, an interesting property of secondary interactions is the ability to form reversible bonds between macromolecules.[24–26] Blending two or more polymer in such a fashion allows the development of new materials that present combined properties of both polymers.[27] Recently, our group has reported the compatibilization of PS and PBMA embedding tetraphosphonate cavitand and *N*-methylpyridinium moiety along the backbone of the polymers.[28] In this work, tetraphosphonate cavitand and *N*-methyl ammonium salt molecules (sarcosine) were randomly copolymerized into the polymer chains of PS and PBMA respectively to investigate the ability of this complex to drive the formation of an amorphous blend. The formation of an homogeneous polymer blend was unambiguously confirmed in solution and at the solid state by complementary analytical tools, namely: NMR, differential scanning calorimetry (DSC) and atomic force microscopy (AFM).

Results and discussion

Self-assembly of the supramolecular homopolymer

Our target monomer was designed placing the sarcosine group at the lower rim of the tetraphosphonate cavitand connected through a short tether, to avoid intramolecular self-association processes. The monomer Tiiii[$3C_3H_7$, 1 sarcosine, CH_3, Ph] (**5**)[29] was synthesized in four steps (22% overall yield, Scheme 1): the key step of the synthesis was the insertion of the Boc-sarcosine moiety at the lower rim of the silyl cavitand **1** under Steglich conditions.[30]

The carbamate protecting group allowed an orthogonal deprotection of the upper rim of **2** using tetra butylammonium fluoride. The four inward phosphonate groups were introduced by reacting the resorcinarene **3** with *P*,*P*-dichlorophenylphosphine and oxidizing the tetraphosphonate intermediate *in situ* with hydrogen peroxide. Finally, cavitand **4** was treated with trifluoroacetic acid to remove the carbamate protecting group and protonate the amine (Scheme 2). Once protonated, this molecule underwent polymerization to the corresponding homopolymer **5**. The intermolecular inclusion process between the methylammonium moiety of one cavitand monomer and the cavity of another was monitored by ^{31}P and ^{1}H NMR spectroscopy. The ^{31}P signal of **4** was split in two singlets because the four phosphorous of the cavitand are not magnetically equivalent (Fig. S1†). After the acidic treatment the ^{31}P signal of the phosphonate groups of the cavitand **5** experienced a downfield shift due to the inclusion of the cationic part of the guest in the cavity. Upon complexation, the methyl protons of the sarcosine group shifted up-field from 2.90 ppm in **4** to −0.7 ppm in **5** (Fig. S2†).[19] These data confirmed the inclusion of the sarcosine group of the monomer within the cavity of another receptor, together with the broadening of all

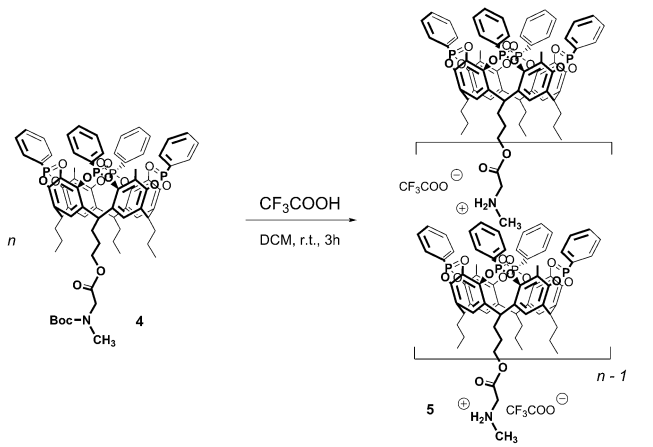

Scheme 2 Formation of homopolymer of Tiiii[$3C_3H_7$, 1 sarcosine salt, CH_3, Ph] (**5**) upon deprotection of precursor **4**.

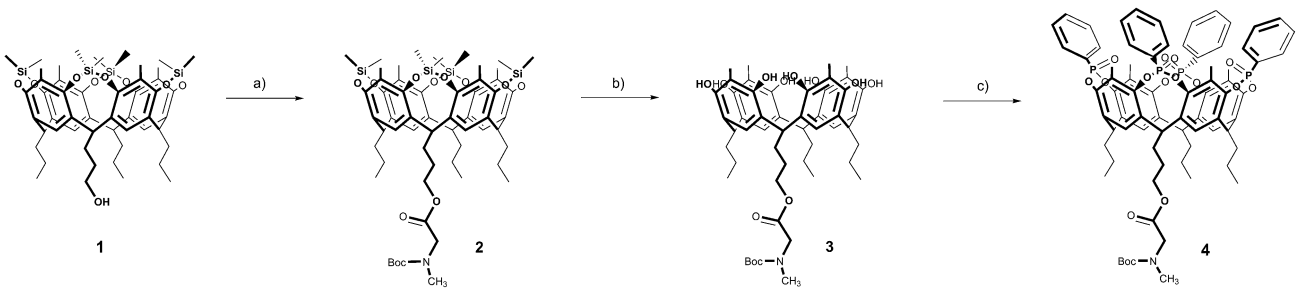

Scheme 1 Synthesis of Tiiii[$3C_3H_7$, 1 sarcosine BOC protected, CH_3, Ph], I: (a) *N*-Boc-sarcosine, DCC/DMAP, $CHCl_3$, r.t., 12 h, 40%; (b) TBAF, THF, r.t., 1 h, 60%; (c) (1) $PhPCl_2$, Py, 75 °C, 3 h; (2) H_2O_2, r.t., 1 h, 92% (over two steps); (d) TFA, DCM, r.t., 3 h, quantitative.

the signals of the ^{1}H NMR spectra – indicating the formation of large aggregates. Quantitative measurement of the association constants (K_{ass}) for Tiiii–guest systems were obtained using isothermal titration calorimetry (ITC). The complexation of sarcosine methyl ester hydrochloride in methanol solution (‡) by the parent Tiiii[C_3H_7, CH_3, Ph] showed a K_{ass} value of 6.8×10^4 M^{-1},[19] while a higher K_{ass} of 2.6×10^6 M^{-1} was measured in dichloromethane for the same cavitand and *N*,*N*-methylbutyl ammonium chloride, that is a proxy for sarcosine (Fig. S3†). To obtain further insights into the self-assembly process, many static (SLS) and dynamic light scattering (DLS) experiments were performed. SLS measurements provided the weight-average molecular weight (M_w) of the aggregates in solution by measuring the intensity of the scattered light. In the case of Tiiii supramolecular homopolymer, SLS measurements were performed in chloroform in the 9.0–40.0 mg mL^{-1} concentration range. Due to the presence of complexation equilibria within the supramolecular polymer, M_w estimations by SLS measurements were made in narrower concentration windows, to have an approximate value of the average molecular weight in the considered concentration regime. In particular the Debye plots for the 9.2–14.1 mg mL^{-1} ($M_w = 7 \pm 1$ kDa) and 25.5–36.7 mg mL^{-1} ($M_w = 11 \pm 1$ kDa) concentration windows are reported in ESI† (Fig. S4 and S5, incremental r. i. $dn/dC = 0.152$ mL g^{-1}, toluene as scattering standard). The DLS experiments on Tiiii homopolymer showed a smooth shifting towards larger size as the concentration was increased – as expected for a supramolecular polymer. Average hydrodynamic diameters starting from 5 nm (2.8 mg mL^{-1}) were obtained, with size distributions showing monodisperse aggregates, with low and reproducible polydispersity index (PdI < 0.2) in the full concentration range that was investigated (Fig. 1). These size distributions found at various concentrations are in agreement with M_w obtained from the SLS data.

SLS and DLS measurements obtained with our instrumentation are – with very good approximation – independent upon the shape of the homopolymer chains in solution, since the measured average hydrodynamic diameter was always lower than 60 nm.[31] The rather narrow degree of polymerization (DP) window (7–11), that can be inferred from these data probably indicates that for Tiiii, the formation of cyclic structures[32] – rather than more longer and flexible linear chains – is strongly favoured, as already demonstrated in the case of A-B supramolecular polymers[32] with similar K_{ass} and given the discrete flexibility of the Tiiii–Tiiii linking.

The size distribution of the homopolymer was also measured at various temperatures to verify the stability of the aggregates (Fig. S6†). These experiments were performed in 1,1,2,2-tetrachloroethane, which has an high boiling point than chloroform, using two different concentrations (4.2 and 36.7 mg mL^{-1}) and a wide range of temperature: for both concentrations we observed stable aggregates with quite low PdI and an hydrodynamic diameter of about 10 nm from 15 °C to 80 °C.

‡ Sarcosine methyl ester hydrochloride is soluble in methanol, not soluble in dichloromethane, chloroform or 1,1,2,2-tetrachloroethane.

Then we turned to investigate the responsive properties of the supramolecular homopolymer employing NMR spectroscopy and DLS (Fig. 2), since homopolymer 5 is able to respond to a simple chemical stimuli such as an acid–base treatment, causing the assembly and disassembly of the aggregates. Compound **5** was easily deprotonated with 3 equivalents of 1,8-diazabicyclo[5.4.0]undec-7-ene (DBU), a non-nucleophilic hindered tertiary amine that, once protonated, does not fit into the receptor cavity. Additionally the deprotonated cavitand can be reconverted to the homopolymer upon subsequent exposure to 5 eq. of trifluoroacetic acid (TFA). The ^{31}P and ^{1}H NMR spectroscopy recorded an high-field shift of the signal after the basic treatment and consequent reappearing of the characteristic pattern of the phosphorous signal similar to that of the protected monomer **5**, while the addition of TFA restored the phosphorous signal at low-field. The pH-responsive properties of the supramolecular homopolymer was also confirmed by DLS studies: as depicted in Fig. 2. DLS size distribution presents a sudden drop of the average hydrodynamic diameter of the homopolymer after the treatment with DBU, with a size consistent with the one of the Tiiii monomer. Subsequently, the addition of TFA restored the initial size distribution demonstrating the reproducible responsiveness of this system. The self-assembly process at 25 °C was also monitored by ^{1}H NMR diffusometry (DOSY, Fig. S6, S8 and S9†). For this analysis, 5.26 mg of Tiiii pre-treated with TFA were dissolved into 750 mL of $CDCl_3$ to give a 5 mM sample (monomer concentration). The diffusion coefficient of the homopolymer in this sample was estimated by means of a LED-STE pulse sequence featuring bipolar gradients of 1 ms duration ($\delta = 2$ ms) and a 100 ms diffusion delay (Δ). The resulting gradient-attenuated transients (32) were processed both by regression fits and by inverse Laplace transform (ILT) of selected peak intensities. Possible convection flow in the 5 mm tube was ruled out by comparing the estimated diffusion coefficient of residual $CHCl_3$ in the sample (2.59×10^{-9} m^2 s^{-1}) with literature data (2.58×10^{-9} m^2 s^{-1}).[33] This analysis provided an apparent diffusion coefficient of 4.22×10^{-10} m^2 s^{-1} for the homopolymer. To minimize the interference from extra NMR signals, the monomers were restored by adding to the previous sample 4 eq. of aqueous NaOD dissolved in MeOD. The resulting mixture was stable over hours, and provided an estimated diffusion coefficient of 2.67×10^{-9} m^2 s^{-1} for residual $CHCl_3$. The apparent diffusion coefficient of the monomer estimated by the same protocol outlined before was 7.49×10^{-10} m^2 s^{-1}, roughly corresponding to a hydrodynamic diameter of 1.0 nm. These data taken in concert, also with the DLS size distribution of the monomer, confirmed that the polymerization degree of the aggregates can be straight forwardly modified altering the pH of the solution.

Compatibilization of two immiscible polymers

Supramolecular self-assembly of the homopolymer has proven that the proposed host–guest interaction is amenable to construct responsive materials driven by non-covalent interactions.

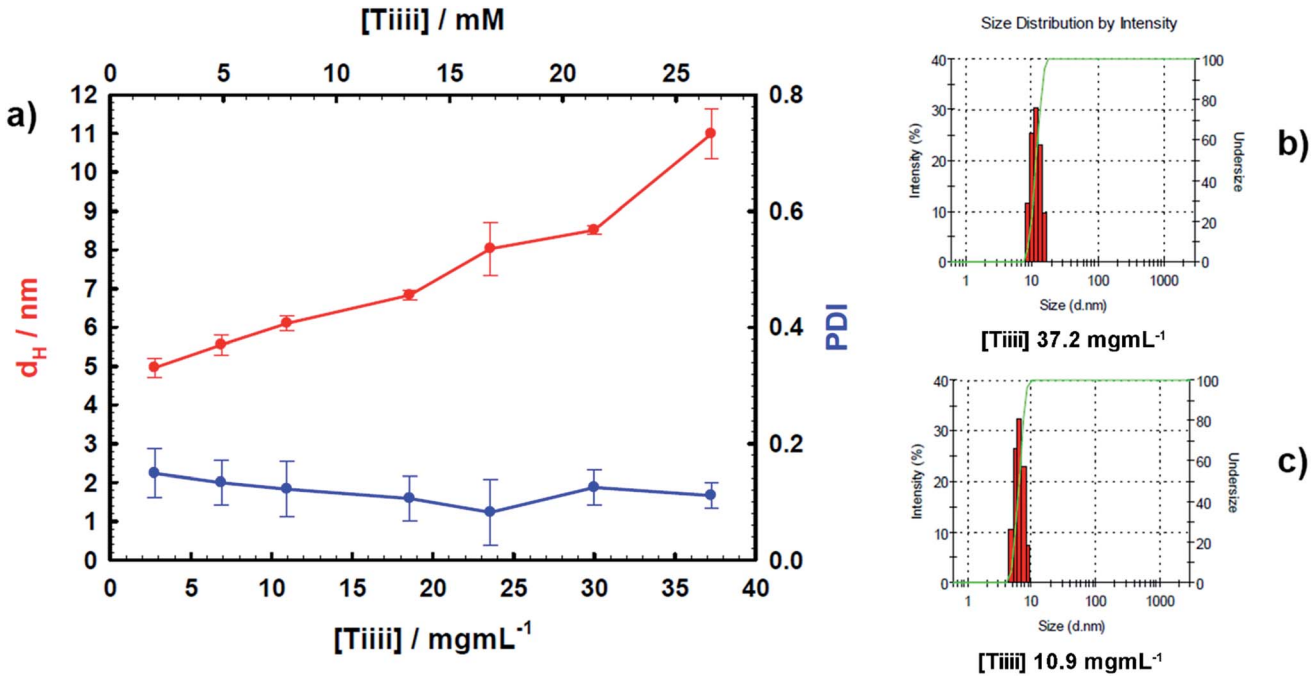

Fig. 1 DLS analysis ($CHCl_3$, 25 °C): (a) hydrodynamic diameter and PDI of the homopolymer **5** as function of concentration; (b) and (c) examples of size intensity distributions at different concentrations.

In this section we test the cavitand–sarcosine hydrochloride binding mode for the compatibilization of two immiscible polymers, namely PS and PBMA. For this purpose we prepared a PS functionalized with tetraphosphonate cavitand (PS–Host, Scheme 3a) and PBMA decorated with a sarcosine hydrochloride moiety (PBMA–Sarc, Scheme 3b). The non-covalent interactions between the host–guest counterparts brought to a cross-link of the polymer chains of the copolymers and consequently the formation of an homogeneous blend. The PS–Host was synthesized and characterized according to protocols previously published by our group.[28]

The PBMA–Sarc was synthesized by copolymerization of butyl methacrylate with the corresponding sarcosine-functionalized monomer, 6-((methylglycyl)oxy)hexyl methacrylate **9**, prepared

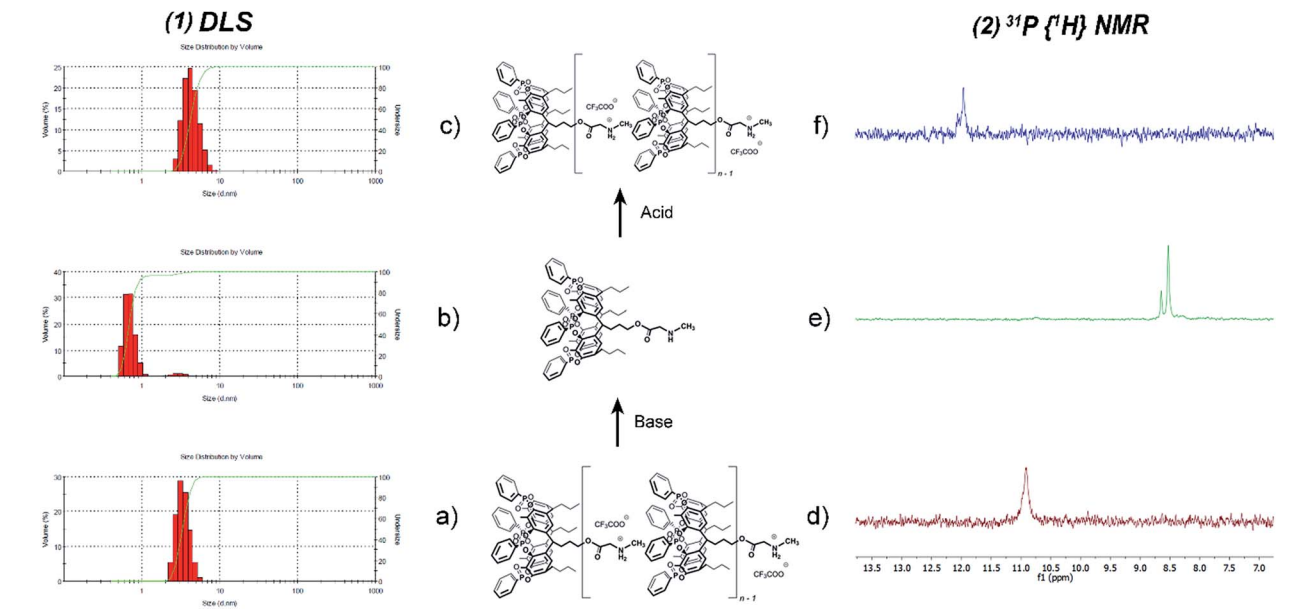

Fig. 2 (1) DLS experiments (hydrodynamic diameter, $CHCl_3$, 10.5 mM, 25 °C): (a) homopolymer; (b) homopolymer + 3 eq. DBU; (c) homopolymer + 3 eq. DBU + 5 eq. triflic acid; (2) $^{31}P\{^1H\}$NMR spectra ($CDCl_3$, 400 MHz, 10 mM, 25 °C) of: (d) homopolymer; (e) homopolymer + 3 eq. DBU; (f) homopolymer + 3 eq. DBU + 5 eq. of TFA.

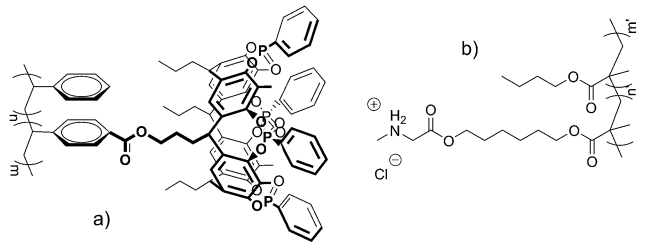

Scheme 3 (a) PS–Host; (b) PBMA–Sarc.

in three steps as reported in Scheme S1.† At first, monoesterification of 1,6-hexanediol with methacryloyl chloride introduced a single methacrylate group, then the monoester was reacted with bromoacetyl chloride using a DCC/DMAP coupling procedure affording the diester **8**. Subsequently, **8** underwent a nucleophilic substitution with methylamine to afford the monomer **9** in 27% overall yield. The free radical copolymerization of **9** with butyl methacrylate followed by treatment with hydrochloric acid afforded the copolymer PBMA–Sarc (Scheme S2†). The ratio between **9** and butyl methacrylate in the reaction was 4 : 96. The polymer was fully characterized by several techniques. ^{1}H NMR (Fig. S10†) spectroscopy and FT-IR (Fig. S11†) assured the formation of the desired copolymer. The percentage of the guest monomer in the copolymer was estimated through elemental analysis and ^{1}H NMR integration. The initial molar composition of butyl methacrylate and **9** was not fully retained inside the polymer. In fact, elemental analysis led to a value of 2.9% molar incorporation. This value was confirmed from ^{1}H NMR integration ratio of the methyl group of sarcosine (2.29 ppm) and OCH_2 groups (3.96 ppm).

The weight-average molecular weight M_w, the number-average molecular weight M_n and the PDI were assessed by gel permeation chromatography (GPC) in chloroform with standard polystyrene calibration. The results are summarized in Table 1 and the refractive index chromatographic trace of **10** is reported in Fig. S12.† The average number of host–guest units per chain (F)[34] was calculated from the experimentally determined monomer molar ratios and M_n of the polymers, obtained respectively by elemental analysis and GPC. Intermolecular association between the two copolymers in solution was monitored by ^{31}P NMR. This technique proved the association between PS–Host and PBMA–Sarc by recording a downfield shift of the phosphorous signal of the cavitand: the 7.8 ppm signal of free PS–Host moved to 11.7 ppm in the presence of PBMA–Sarc (Fig. S13†). The ^{31}P NMR analysis indicated that the F values reported in Table 1 are correct for the determination of the 1 : 1 host–guest molar ratio between the two polymers. The next step was to study the blend at the solid state: PS–Host and PBMA–Sarc were dissolved in dichloromethane and the two solutions were mixed together in the right proportion to obtain a 1 : 1 molar ratio of cavitand hosts and sarcosine hydrochloride guests attached to the polymer backbone (see Experimental section). The miscibility of the two copolymers was assessed using two different methods, differential scanning calorimetry (DSC) on the powder and atomic force microscopy (AFM) on spin cast films. Materials formed by a single phase structure exhibit only one glass transition temperature (T_g) that can be determined *via* DSC.[35] The 1 : 1 molar mixture of PS–Host and PBMA–Sarc showed one endothermic relaxation peak, in between the T_g of the two functionalized polymers, indicative of an homogeneous blend (Table 2, Fig. 3 and S14†).

AFM experiments were performed in contact mode on spin cast films to determine the morphological homogeneity of the mixture of PS–Host and PBMA–Sarc. It is well known that in case of films prepared from blends of immiscible polymers, the topography consists of segregated islands and depressions, while on the contrary, a flat and homogeneous surface indicates good miscibility of the polymers. In the pristine PBMA/PS mixture, PBMA, having higher mobility, migrate to the silicon surface, while PS tends to segregate forming the islands above PBMA. The phase segregation results from the combination of the low chemical affinity between the two polymers, and the great difference in terms of their surface energy.[36] A thin film was prepared from a 0.5 mM solution of a 1 : 1 molar mixture of PS–Host and PBMA–Sarc and was deposited on Si/SiO_x surface by spin coating (1500 rpm for 30 s, dichloromethane as solvent). As the T_g of the two polymers are completely different (PS $\sim$ 100 °C, PBMA $\sim$ 23 °C), it was necessary to work at 15 °C, to avoid any dewetting-related phenomenon.

Fig. 4a shows a typical morphology corresponding to the immiscible PS–PBMA blend, while Fig. 4b, by contrast, reports the homogeneous and flat topographic image of compatibilized PS–Host and PBMA–Sarc blend. These two evidences

Table 2 Glass transition temperatures of copolymers PS–Host, PB–Sarc and mixture

Polymers	T_g (°C)
PS–Host	97.1
PBMA–Sarc	14.6
PS–Host/PBMA–Sarc	37.3

Table 1 GPC characterization of the polymers and average number of host–guest units F

Polymers	M_n[a]	M_w[a]	PDI[a]	mol% F units[b]	Average no. of F units per chain[c]
PS–Host-4%	20 800	27 100	1.30	3.9	5.3
PBMA–Sarc-4%	23 200	36 600	1.58	2.9	4.6

[a] Relative molecular weights against PS standards obtained from GPC in $CHCl_3$. [b] Determined by elemental analyses and ^{1}H NMR integration. [c] Calculated from the number-average molecular weights ($\overline{M_n}$) and mol% recognition unit of the polymers.

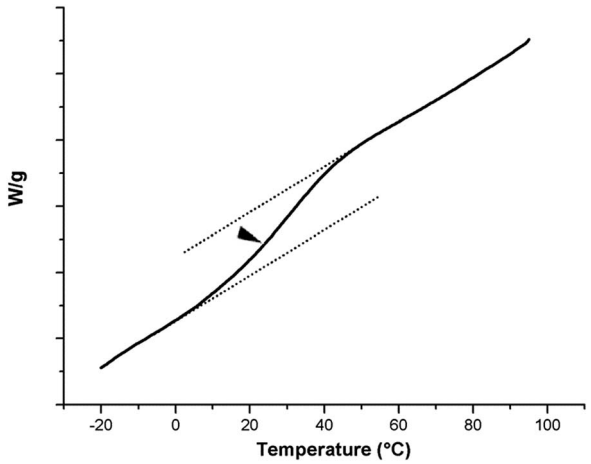

Fig. 3 DSC thermogram of 1 : 1 molar mixture PS–Host/PBMA–Sarc.

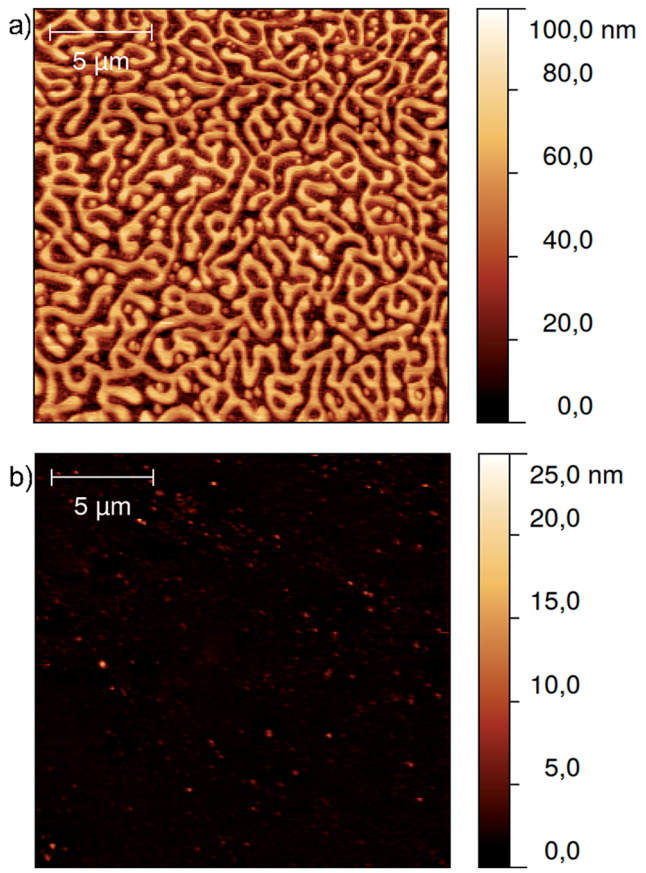

Fig. 4 (a) AFM topographic image of PS/PBMA mixture, deposited by spin coating of a dichloromethane solution, displaying large lateral in homogeneities; (b) the same for a film made of 1 : 1 molar mixture PS–Host/PBMA–Sarc, exhibiting an homogeneous and flat morphology.

demonstrate the mixing of the two copolymers at the molecular level, hence their compatibilization driven by host–guest interactions between the cavitand and the sarcosine hydrochloride units, present in low amounts in the two copolymers.

Conclusions

In summary, the molecular recognition properties of the tetraphosphonate cavitand/*N*-methyl ammonium complex were successfully translated in supramolecular polymer chemistry in two different settings. By first a new stimuli responsive supramolecular homopolymer were designed and synthesized, exploiting the monomer Tiiii[$3C_3H_7$, 1 sarcosine, CH_3, Ph] as building block based on the resorcinarene scaffold, and presenting four P═O groups at the upper rim and a sarcosine moiety at the lower rim. The self-assembly properties of this supramolecular polymer were investigated with several techniques which provided numerous evidences on the formation of supramolecular homopolymer in solution. Furthermore, the polymers assembly was controlled by means of acid–base treatment demonstrating the reversibility of the system. In the second study, the host–guest counterpart was embedded in polymeric materials to test its ability to promote polymer blending. The formation of an homogeneous blend was unambiguously confirmed by several and complementary analytical tools, such as NMR, DSC and AFM. The precise response to pH constitutes a significant advantage for controlling and driving polymer blending. The present findings lead us to propose this pH responsive host–guest system as an useful tool to manipulate the properties of polymeric species and to generate pH responsive polymeric interfaces.

Experimental section

Materials and methods

All reagents and chemicals were obtained from commercial sources and used without further purification. Compound **1** was prepared according to the published procedure.[37] Dry pyridine was distilled from KOH before use. *n*-Butyl methacrylate (Aldrich) was distilled under vacuum to remove stabilizers. 2,2′-Azobis(2-methylpropionitrile) (AIBN, Fluka), was purified by crystallization in acetone. Column chromatography was performed using silica gel 60 (MERCK 70-230 mesh). Electrospray ionization ESI-MS experiments were performed on a Waters ZMD spectrometer equipped with an electrospray interface. Exact masses were determined using a LTQ ORBITRAP XL Thermo spectrometer equipped with an electrospray interface. MALDI-TOF spectra was performer using AB SCIEX MALDI TOF-TOF 4800 Plus (matrix: α-cyano-4-hydroxycinnamic acid). ^{1}H NMR spectra were obtained using a Bruker AVANCE-300 (300 MHz) or a Bruker AVANCE 400 (400 MHz). All chemical shifts (δ) were reported in ppm relative to the proton resonances resulting from incomplete deuteration of the NMR solvents. ^{31}P NMR spectra were obtained using a Bruker AVANCE-400 (162 MHz) spectrometer. All chemical shifts (δ) were recorded in ppm relative to external 85% H_3PO_4 at 0.00 ppm. FT-IR spectra were recorded on a Perkin Elmer FT-IR Spectrum One Spectrometer on films obtained by solution casting onto KBr windows of polymers diluted $CHCl_3$ solution. DSC thermograms were recorded by using a Mettler Toledo Stare System, model DSC 822e differential scanning calorimeter equipped with a Stare software.

AFM measurements

Surface topography was examined using an atomic force microscope Thermomicroscope Autoprobe CP Research. All measurements were performed either in contact mode or in tapping mode employing respectively Silicon Nitride probes (Veeco OTR4-35, typical spring constant 0.05 N m^{-1}) or silicon probes (Bruker, MPP-12100, typical spring constant 3 N m^{-1}), and to preserve the initial structure, the films were not annealed. Given the low T_g of PBMA, to minimize artifacts due to tip-sample interactions, all samples were measured at 15 °C using a Peltier cell in a dry chamber to prevent humidity condensation. The collected images were analyzed using the proprietary software or Gwyddion, an Open Source software, covered by GNU General Public License (http://Gwyddion.net).

GPC measurements

GPC System apparatus equipped with Jasco PU-2089 Plus pump, Jasco RI 2031 Plus as Refractive Index Detector, Jasco CO_2063 Plus column oven (set at 30 °C) and 2 polymer laboratories PL gel MIXED D columns and PL gel guard column poly(styrene-*co*-divinylbenzene) (linear range 100–600 000 Da), was used for determination of molecular weight of chloroform diluted solutions of samples (eluted at 1 mL min^{-1}). The calibration curve was made with polystyrene standards and calculations were carried out with software Borwin 1.21.61 (JMBS DEVELOPMENT).

Light scattering measurements

SLS and DLS measurements were performed using a Malvern Nano ZS instrument, equipped with a 633 nm laser source. All the solution were filtered with PTFE filters (4 mm × 0.2 μm, Supelco). The width of DLS hydrodynamic diameter distribution is indicated by PdI (Polydispersion Index). In case of a mono-modal distribution (gaussian) calculated by means of cumulant analysis, $PdI = (\sigma/Z_{avg})^2$, where σ is the width of the distribution and Z_{avg} is average diameter of the particles population respectively.

Polymer blending and film deposition

Solutions of the different polymers (0.5 mM) in CH_2Cl_2 were prepared. PS–Host-4% (42 mg) was dissolved in 4 mL of CH_2Cl_2, whereas 40 mg of PBMA–Sarc-4% were dissolved in 4 mL of CH_2Cl_2. 1 mL aliquot of PS–Host solution was mixed with 1.38 mL of PBMA–Sarc solution, and 100 μL of the resulting solution was filtered over 0.45 μm PTFE filter and spin-coated on a silicon slice at 1500 rpm for 30 seconds. The films were analyzed without any further modification.

NMR diffusometry

NMR diffusometry experiments were performed on a Bruker AVANCE III (500 MHz) spectrometer equipped with a BBI Z-gradient probe (max. gradient = 55 G cm^{-1}). DOSY maps were obtained with Bruker Dynamics Center 2.2.1 after spectra pre-processing in TopSpin 3.1. Both fitting and inverse Laplace transform (ILT) methods were employed to check for consistency of the results. The final values for the apparent diffusion coefficients (free and oligomer) were obtained by averaging the values relative to selected signals.

N-Boc-sarcosine

To a solution of sarcosine (0.4 g, 4.49 mmol) in acetonitrile, triethylamine (0.68 mL, 4.94 mmol) and di-*tert*-butyl dicarbonate (1.13 mL, 4.94 mmol) were added. The solution was heated to reflux for 4 hours and the solvent removed *in vacuo*. The crude oil was dissolved in dichloromethane and extracted with water (2 × 30 mL). The organic phase was dried with anhydrous $CaCl_2$ and evaporated under reduced pressure to give the product as colorless oil (0.4 g, 2.15 mmol, 48%). ^{1}H NMR ($CDCl_3$, 400 MHz): δ (ppm) = 9.56 (s, 1H, OH), 3.87 (d, J = 33.4 Hz, 2H, NCH_2), 2.83 (s, 3H, NCH_3), 1.34 (s, 9H, $C(CH_3)_3$); ESI-MS: m/z 190.1 $[M + H]^+$.

N-Boc-sarcosine based silyl-cavitand (2)

N-Boc-sarcosine (0.31 g, 1.68 mmol), DCC (0.34 g, 1.68 mmol) and DMAP (0.2 g, 1.68 mmol) were dissolved in dry chloroform under stirring for 15 minutes. Successively, monohydroxy footed silylcavitand **1** (0.8 g, 0.83 mmol) was added into the reaction mixture and stirred overnight at room temperature. Saturated NH_4Cl solution was added and the organic phase was extracted with water (2 × 20 mL) dried with anhydrous Na_2SO_4, filtered and the solvent was removed *in vacuo*. Purification by silica gel column chromatography (hexane : ethyl acetate 85 : 15) yielded the desired product as white solid (0.37 g, 0.33 mmol, 40%). ^{1}H NMR ($CDCl_3$, 300 MHz): δ (ppm) = 7.20 (s, 2H, ArH), 7.18 (s, 2H, ArH), 4.64 (t, ^3J = 8 Hz, 4H, ArCH), 4.28–4.20 (m, 2H, $CH_2OC(O)$), 3.96 (d, J = 40 Hz, 2H, NCH_2), 2.85 (d, J = 10.3 Hz, 3H, NCH_3), 2.27–2.01 (m, 10H, $CH_2CH_2CH_2OC(O)$, $CH_2CH_2CH_3$), 1.85 (s, 12H, $ArCH_3$); 1.67–1.14 (m, 17H, $CH_2CH_2OC(O)$, $C(CH_3)_3$, $CH_2CH_2CH_3$), 0.98–0.82 (m, 9H, $CH_2CH_2CH_3$), 0.54 (s, 12H, $SiCH_{3,out}$), −0.64 (s, 12H, $SiCH_{3,in}$); ESI-MS: m/z 1164.1 $[M + K]^+$.

N-Boc-sarcosine based resorcinarene (3)

To a solution of *N*-Boc-sarcosine based silyl-cavitand **2** (0.39 g, 0.34 mmol) in dry THF, TBAF (1.36 g; 5.2 mmol) was added under argon atmosphere at 0 °C. After 1 hour the reaction mixture was quenched by adding saturated NH_4Cl solution, the crude mixture was diluted with ethyl acetate and the organic phase was extracted with sat. aq. $NaHCO_3$ and water. The organic phase was dried with anhydrous Na_2SO_4 and the solvent removed *in vacuo*. Purification by silica gel column chromatography (hexane : ethyl acetate 1 : 1) afforded the pure product as yellow pale solid (0.18 g, 0.2 mmol, 60%). ^{1}H NMR ($(CD_3)_2CO$, 300 MHz): δ (ppm) = 7.84 (s, 2H, OH), 7.46 (s, 2H, ArH), 7.44 (s, 2H, ArH), 4.41 (t, ^3J = 9 Hz, 4H, ArCH), 4.24–4.11 (m, 2H, $CH_2OC(O)$), 3.97 (d, J = 14.5 Hz, 2H, NCH_2), 2.91 (d, J = 9 Hz, 3H, NCH_3), 2.45–2.00 (m, 20H, $CH_2CH_2CH_2OC(O)$, CH_2CH_2-CH_3, $ArCH_3$), 1.71–1.55 (m, 2H, $CH_2CH_2OC(O)$), 1.50–1.18 (m, 15H, $C(CH_3)_3$, $CH_2CH_2CH_3$), 0.95 (t, ^3J = 9 Hz, 9H, $CH_2CH_2CH_3$); ESI-MS: m/z 922.8 $[M + Na]^+$, 939 $[M + K]^+$.

Tiiii[3C_3H_7, 1 Boc-sarcosine, CH_3, Ph] (4)

To a solution of *N*-Boc-sarcosine based resorcinarene **3** (0.19 g, 0.21 mmol) in freshly distilled pyridine, dichlorophenylphosphine (0.13 mL, 0.88 mmol) was slowly added at room temperature under argon atmosphere. After 3 hours of stirring at 75 °C, the solution was allowed to cool at room temperature and aqueous H_2O_2 (2 mL, 30%) was added. The resulting mixture was stirred for 1 hour at room temperature, then addition of water resulted in the precipitation of a white powder. The solid was recovered by suction filtration to give pure **4** (0.45 g, 0.33 mmol, 92%). ^{1}H NMR ($CDCl_3$, 400 MHz): δ (ppm) = 8.15–8.01 (m, 8H, P(O)ArH_o), 7.72–7.61 (m, 4H, P(O)ArH_p), 7.61–7.47 (m, 8H, P(O)ArH_m), 7.24–7.13 (m, 4H, ArH), 4.85–4.72 (m, 4H, ArCH), 4.35–4.24 (m, 2H, CH_2OC(O)), 3.97 (d, J = 36 Hz, 2H, NCH_2), 2.90 (s, 3H, NCH_3), 2.44–2.21 (m, 8H, $CH_2CH_2CH_3$, $CH_2CH_2CH_2$OC(O)), 2.14 (s, 12H, ArCH_3), 1.82–1.69 (m, 2H, CH_2CH_2OC(O)), 1.50–1.21 (m, 15H, C(CH_3)$_3$, $CH_2CH_2CH_3$), 1.12–0.98 (m, 9H, $CH_2CH_2CH_3$); ^{31}P ^{1}H NMR ($CDCl_3$, 161.9 MHz): δ (ppm) = 8.44 (s, 1P, P═O) 8.34 (s, 3P, P═O); HR-ESI-MS: *m*/*z* calcd for $C_{76}H_{81}NO_{16}P_4Na$: 1410.4403; found: 1410.4398.

Tiiii[3C_3H_7, 1 sarcosine salt, CH_3, Ph] (5)

Cavitand **4** (20 mg, 0.014 mmol) was treated with 10 equivalent of trifluoroacetic acid in $CHCl_3$. After 3 hours the solvent was removed *in vacuo* and the crude was dried under reduced pressure (quantitative yield). ^{1}H NMR ($CDCl_3$, 400 MHz): δ (ppm) = 8.17–7.96 (m, 8H, P(O)ArH_o), 7.89–7.42 (m, 16H, P(O)ArH_p, P(O)ArH_m, ArH), 4.85–4.61 (m, 4H, ArCH), 4.25 (s, 2H, CH_2OC(O)), 3.30 (s, 2H, NCH_2), 2.66–2.30 (m, 8H, $CH_2CH_2CH_3$, $CH_2CH_2CH_2$OC(O)), 2.14 (s, 12H, ArCH_3), 1.79–1.59 (m, 2H, CH_2CH_2OC(O)), 1.51–1.20 (m, 8H, $CH_2CH_2CH_3$), 1.16–0.81 (m, 9H, $CH_2CH_2CH_3$), −0.68 (s, 3H, NCH_3); ^{31}P ^{1}H NMR ($CDCl_3$, 161.9 MHz): δ (ppm) = 11.01 (s, P═O); MALDI TOF-TOF: calcd for $C_{71}H_{74}NO_{14}P_4$ 1288.4054 Da, found: 1288.3879 Da.

Acknowledgements

We thank the Centro Interfacoltà di Misure "G. Casnati" of the University of Parma for the use of AFM, MS and NMR facilities. D. M. thanks the EU through FP7 Project DIRAC (SEC-2009-242309) for partial support of his scholarship. F.R. acknowledges financial support from project PRAT CPDA132473/13 granted by Università degli Studi di Padova.

Notes and references

1 R. J. Wojtecki, M. A. Meador and S. J. Rowan, *Nat. Mater.*, 2011, **10**, 14.
2 T. Aida, E. W. Meijer and S. I. Stupp, *Science*, 2012, **335**, 813.
3 L. Brunsveld, B. J. B. Folmer, E. W. Meijer and R. P. Sijbesma, *Chem. Rev.*, 2001, **101**, 4071.
4 A. Harada, Y. Takashima and M. Nakahata, *Acc. Chem. Res.*, 2014, **47**, 2128.
5 J. del Barrio, P. N. Horton, D. Lairez, G. O. Lloyd, C. Toprakcioglu and O. A. Scherman, *J. Am. Chem. Soc.*, 2013, **135**, 11760.
6 Y. Liu, H. Yang, Z. Wang and X. Zhang, *Chem.–Asian J.*, 2013, **8**, 1626.
7 Y. Liu, Y. Yu, J. Gao, Z. Wang and X. Zhang, *Angew. Chem., Int. Ed.*, 2010, **49**, 6576.
8 C. Capici, Y. Cohen, A. D'Urso, G. Gattuso, A. Notti, A. Pappalardo, S. Pappalardo, M. F. Parisi, R. Purrello, S. Slovak and V. Villari, *Angew. Chem., Int. Ed.*, 2011, **50**, 11956.
9 D.-S. Guo and Y. Liu, *Chem. Soc. Rev.*, 2012, **41**, 5907.
10 M. Zhang, X. Yan, F. Huang, Z. Niu and H. W. Gibson, *Acc. Chem. Res.*, 2014, **47**, 1995.
11 B. Zheng, F. Wang, S. Dong and F. Huang, *Chem. Soc. Rev.*, 2012, **41**, 1621.
12 Z. Zhang, Y. Luo, J. Chen, S. Dong, Y. Yu, Z. Ma and F. Huang, *Angew. Chem., Int. Ed.*, 2011, **50**, 1397.
13 P. Wei, B. Xia, Y. Zhang, Y. Yu and X. Yan, *Chem. Commun.*, 2014, **50**, 3973.
14 B. Xia, B. Zheng, C. Han, S. Dong, M. Zhang, B. Hu, Y. Yu and F. Huang, *Polym. Chem.*, 2013, **4**, 2019.
15 X. Yan, F. Wang, B. Zheng and F. Huang, *Chem. Soc. Rev.*, 2012, **41**, 6042.
16 F. Tancini, R. M. Yebeutchou, L. Pirondini, R. De Zorzi, S. Geremia, O. A. Scherman and E. Dalcanale, *Chem.–Eur. J.*, 2010, **16**, 14313.
17 R. M. Yebeutchou, F. Tancini, N. Demitri, S. Geremia, R. Mendichi and E. Dalcanale, *Angew. Chem., Int. Ed.*, 2008, **47**, 4504.
18 M. Dionisio, G. Oliviero, D. Menozzi, S. Federici, R. M. Yebeutchou, F. P. Schmidtchen, E. Dalcanale and P. Bergese, *J. Am. Chem. Soc.*, 2012, **134**, 2392.
19 E. Biavardi, C. Tudisco, F. Maffei, A. Motta, C. Massera, G. G. Condorelli and E. Dalcanale, *Proc. Natl. Acad. Sci. U. S. A.*, 2012, **109**, 2263.
20 C. Tudisco, F. Bertani, M. T. Cambria, F. Sinatra, E. Fantechi, C. Innocenti, C. Sangregorio, E. Dalcanale and G. G. Condorelli, *Nanoscale*, 2013, **5**, 11438.
21 P. Delangle, J.-C. Mulatier, B. Tinant, J.-P. Declercq and J.-P. Dutasta, *Eur. J. Org. Chem.*, 2001, **2001**, 3695.
22 E. Kalenius, D. Moiani, E. Dalcanale and P. Vainiotalo, *Chem. Commun.*, 2007, 3865.
23 M. Melegari, M. Suman, L. Pirondini, D. Moiani, C. Massera, F. Ugozzoli, E. Kalenius, P. Vainiotalo, J.-C. Mulatier, J.-P. Dutasta and E. Dalcanale, *Chem.–Eur. J.*, 2008, **14**, 5772.
24 J. M. G. Cowie and A. Demaude, *Polym. Adv. Technol.*, 1994, **5**, 178.
25 M. C. Piton and A. Natansohn, *Macromolecules*, 1995, **28**, 1605.
26 J. Shen and T. Hogen-Esch, *J. Am. Chem. Soc.*, 2008, **130**, 10866.
27 Y. S. Lipatov, *Prog. Polym. Sci.*, 2002, **27**, 1721.
28 M. Dionisio, L. Ricci, G. Pecchini, D. Masseroni, G. Ruggeri, L. Cristofolini, E. Rampazzo and E. Dalcanale, *Macromolecules*, 2014, **47**, 632.

29 R. Pinalli, M. Suman and E. Dalcanale, *Eur. J. Org. Chem.*, 2004, **2004**, 451.
30 B. Neises and W. Steglich, *Angew. Chem., Int. Ed.*, 1978, **17**, 522.
31 Sample measurements performed to demonstrate Zetasizer performance, Technical Note, Malvern Instruments Limited, 2014, pp. 15–16.
32 T. F. A. de Greef, G. Ercolani, G. B. W. L. Ligthart, E. W. Meijer and R. P. Sijbesma, *J. Am. Chem. Soc.*, 2008, **130**, 13755.
33 D. W. McCall and D. C. Douglass, *J. Phys. Chem.*, 1967, **71**, 987.
34 T. Park and S. C. Zimmerman, *J. Am. Chem. Soc.*, 2006, **128**, 11582.
35 M. Aubin and R. E. Prud'homme, *Macromolecules*, 1988, **21**, 2945.
36 C. Chen, J. Wang, S. E. Woodcock and Z. Chen, *Langmuir*, 2002, **18**, 1302.
37 F. Hauke, A. J. Myles and J. Rebek Jr, *Chem. Commun.*, 2005, 4164.